EGJ Engineering Geology of Japan

Detrital zircon geochronology of sandstones from Jurassic and Cretaceous accretionary complexes in the Kanto Mountains, Japan: implications for arc provenance

Kazumasa Aoki [1)]*, Yukio Isozaki [2)], Shuhei Sakata [3)], Tomohiko Sato [4)], Shinji Yamamoto [2)] and Takafumi Hirata [3)]

Abstract In order to obtain information about provenance of terrigenous clastics that make up most of the Jurassic-Cretaceous accretionary complex (AC) of SW Japan, we have conducted detrital zircon U-Pb dating (laser-ablation inductively coupled plasma-mass spectrometry - LA-ICP-MS) of two Jurassic sandstones and four Cretaceous sandstones from the Mitsumine area, Kanto Mountains near Tokyo. Except for one sample, the youngest U-Pb age data obtained from each sample are 159.6 ± 4.9, 122.7 ± 3.8, 97.5 ± 2.3, 96.7 ± 4.3 and 87.7 ± 1.9 Ma that are consistent with microfossil ages previously reported from shales in the same units, confirming the polarity of tectonic-downward growth of the ACs across the Butsuzo Tectonic Line, previously estimated from biostratigraphic dating. The new zircon U-Pb age data also reveal that the Jurassic and Cretaceous sandstones contain many ca. 200-160 Ma and ca. 120-90 Ma detrital zircons, respectively. These results indicate that granitic arc-batholiths corresponding to each age were widely exposed in the fore-arc region when the sandstones were deposited. Detrital zircon data including this study have revealed that the Late Jurassic and Cretaceous sandstones are significantly low in population of Proterozoic ages than the Middle Jurassic sandstone, suggesting that a major provenance shift occurred between middle and late Jurassic. Arc batholith formation derived from oceanic-plate subduction typically causes high topographic relief in a fore-arc. Thus, it is likely that the formation of the granitic batholiths played an important role in the provenance shift, which had an important effect on the supply of terrigenous clastics in the Jurassic-Cretaceous fore-arcs in Japan. The large amount of Late Jurassic and Cretaceous batholiths might serve as barriers to restrict the supply route of the terrigenous clastics from the back-arc side.

Keywords: accretionary complex, zircon, U-Pb age

1. Introduction

Jurassic and Cretaceous accretionary complexes (ACs) are widely exposed in the Mitsumine area of the Kanto mountains, central Japan (Fig. 1). The ACs were subdivided into multiple units based on differences in their lithofacies, structures and fossil ages (e.g. Fujimoto *et al.*, 1950; Hisada, 1984; Matsuoka *et al.*, 1998; Takahashi, 2000; Hara *et al.*, 1998, 2010). However, there are still no detrital zircon U-Pb ages of terrigenous clastic rocks of these AC units. Detrital zircon U-Pb data from terrigenous rocks can be used to constrain their tectono-sedimentary development (e.g. Dickinson and Gehrels, 2008; Clift *et al.*, 2009; Isozaki *et al.*, 2010; Aoki *et al.*, 2012; 2014; LaMaskin, 2012; Okawa *et al.*, 2013). Hence, detrital zircon data from this area are widely expected to contribute to an improved understanding of the tectonic development of the Jurassic-Cretaceous ACs in Japan. In this study, we conducted detrital zircon U-Pb analyses of sandstones from two Jurassic and four Cretaceous

*Corresponding author: Kazumasa Aoki
E-mail: kazumasa@das.ous.ac.jp
1) Department of Applied Science, Okayama University of Science, 1-1 Ridai-cho, Kita-ku, Okayama 700-0005, Japan
2) Department of Earth Science and Astronomy, The University of Tokyo, 3-8-1 Komaba, Meguro-ku, Tokyo 153-8902, Japan
3) Department of Geology and Mineralogy, Kyoto University, Kitashirakawaoiwake-cho, Sakyo-ku, Kyoto 606-8502, Japan
4) Earth-Life Science Institute, Tokyo Institute of Technology, 2-12-1 Ookayama, Meguro-ku, Tokyo 152-8551, Japan

Received on April 17, 2015; Accepted on June 5, 2015.

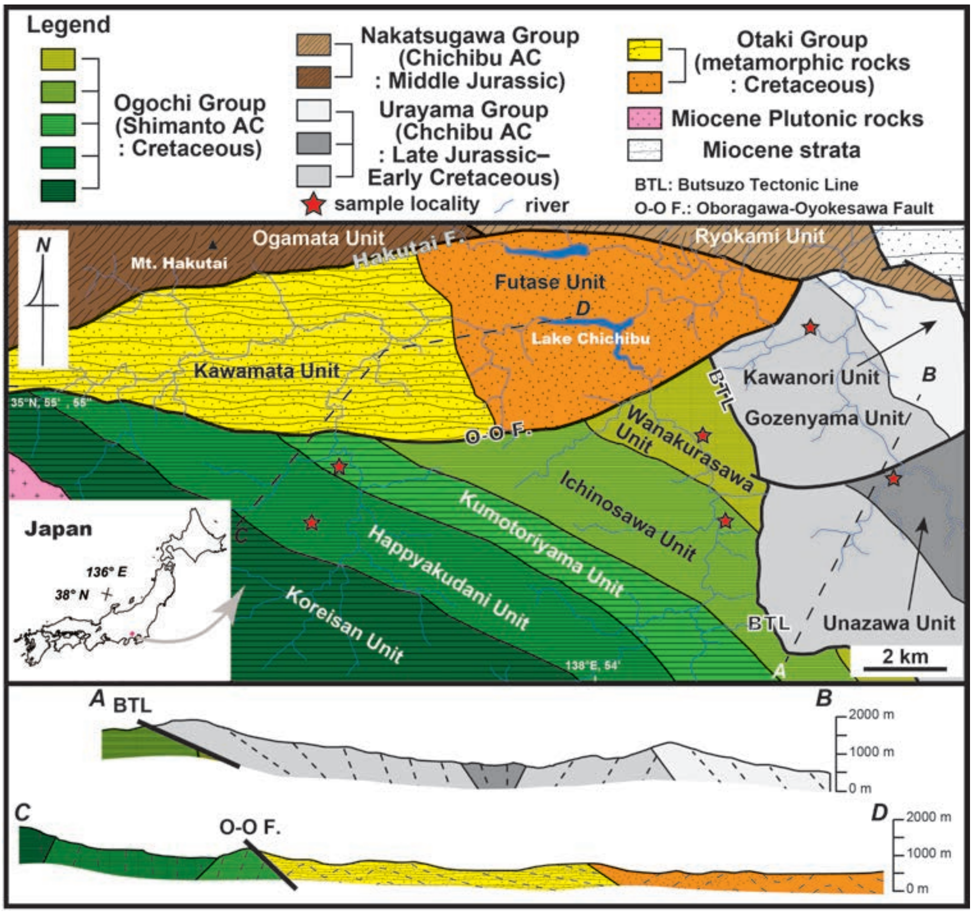

Fig. 1 (A) Distribution of Jurassic and Cretaceous ACs in the Mitsumine area, Kanto Mountains, central Japan (modified from Hara *et al*., 2010). Schematic cross-sections along A-B and C-D in the main map are also shown.

accretionary units in the Mitsumine area, using laser-ablation inductively coupled plasma-mass spectrometry (LA-ICP-MS). The name of each unit follows the classification by Hara *et al* (2010) and the geologic time scale that of Gradstein *et al* (2012).

2. Geologic outline

The Jurassic AC (Chichibu belt) and the Cretaceous AC (Shimanto belt) extend from the Kanto district to the Ryukyu Islands for over 1800 km along the Pacific side of SW Japan (e.g. Isozaki and Nishimura, 1989; Isozaki, 1996). These belts are basically characterized by an oceanward-vergent fold-and-thrust structures, and their biostratigraphic ages become younger oceanwards and structurally downwards. These ACs mainly comprise imbricated thrust sheets that internally retain "Ocean Plate Stratigraphy (OPS)" (e.g. Matsuda and Isozaki, 1991; Kusky *et al*., 2013) and chaotically-mixed mélange units. The mélange units consist of blocks and slivers of basalt and chert with sandstone and mudstone matrix; see Taira *et al*. (1988), Isozaki, (1996, 1997), Kimura (1997) and Isozaki *et al*. (2010) for more detailed basic geological information of these ACs.

The Jurassic AC in the Mitsumine area is divisible into two geologic groups, which are bounded by the east-west tending Hakutai Fault (Chichibu Geologic Research Group, 1966). On the north side of the fault is the Nakatsugawa Group (Middle Jurassic), and on the south side is the Urayama Group (Late Jurassic-Early Cretaceous). Both groups consist mainly of sandstone, mudstone siliceous mudstone, chert, limestone, and greenstone (Hara *et al*., 2010). The Urayama group is subdivided into three units (Kawanori, Unazawa and Gozenyama) from top to bottom separated by thrust boundaries (Hisada, 1984; Hara *et al*., 2010); these three units mostly strike N40-60°W and dip 60-70°N or S. Hara and Hisada (2005) reported K-Ar illite ages of 76-71 Ma from phyllites in the Gozenyama Unit. Our analyzed sandstone samples were collected from the Unazawa Unit (sample no. KV13-7, lat/long: 35°N, 54', 30.62", 138°E, 58', 31.83") and Gozenyama Unit (KV13-8: 35°N, 56', 25.31", 138°E, 57', 26.74") (Fig. 1).

To the southwest of the Butsuzo Tectonic line (BTL) or to the south of the Oboragawa-Oyokesawa Fault, a Middle-Late Cretaceous AC within the Ogochi Group is widespread in the Mitsumine area (e.g. Iyota *et al*., 1994;

Hara *et al.*, 2010) (Fig. 1). This Group commonly strikes N 40-70°W and dips 60-80°N or S, and is subdivided into the Wanakurasawa, Ichinosawa, Kumotoriyama, Happyakudani and Koreisan units in descending order (Fig. 1), which are all separated by thrusts. Their main constituent rocks are sandstone and mudstone with minor greenstone, chert and limestone (e.g. Hara *et al.*, 2010). For this study we collected sandstone samples from the Wanakurasawa (KV13-4: 35°N, 54', 58.34", 138°E, 55', 45.39"), Ichinosawa (KV13-2: 35°N, 53', 55.64", 138°E, 56', 2.86"), Kumotoriyama (KV13-14: 35°N, 54', 33.82", 138°E, 49', 59.05") and Happyakudani (KV13-13: 35°N, 54', 2.22", 138°E, 49', 35.92") units (Fig. 1). Hara *et al.* (2010) provides more detailed geology of the Mitsumine area. In addition, we collected meta-sandstone samples from the Futase and Kawamata units (see Fig. 1), which were affected by Cretaceous greenschist facies metamorphism (Ogawa *et al.*, 1988; Hara *et al.*, 1998; Hara and Hisada, 2005, 2007); the age data from these two units will be published later.

3. Zircon separation and analytical procedures

Detrital zircon grains separated from each sample were mounted on a 5 mm acrylic disc and appropriately polished. Most are colorless and euhedral with average lengths ca. 130 μm. Most zircons exhibit oscillatory growth zoning from core to rim in cathodoluminescence (CL) image (Fig. 2). We dated the igneous oscillatory-zoned parts of each grain (e.g. Corfu *et al.*, 2003).

In situ zircon U-Pb dating was carried out with a Nu AttoM single-collector ICP-MS (Nu instruments, Wrexham, UK) coupled to a NWR-193 laser-ablation system (ESI, Portland, US) that utilizes a 193 nm ArF excimer laser at the Department of Geology and Mineralogy, Kyoto University. Detailed analytical procedures are given in Appendix A.

4. Results

The LA-ICP-MS U-Pb dating of individual zircon grains provided 46, 56, 58, 42, 53 and 66 concordia data from samples KV13-7, KV13-8, KV13-4, KV13-2, KV13-14 and KV13-13, respectively (Appendix Tables 2-7). To avoid analytical bias owing to lead loss/addition, discordant measurements (over 10% discordance) were removed. Figure 4 shows $^{206}Pb/^{238}U$ age histograms of detrital zircons with probability age frequency curves that were made with Isoplot/Ex 3 (Ludwig, 2003).

4.1. Urayama Group

The age frequency curve for sandstone (KV13-7) from the Unazawa Unit shows three clusters of ages:

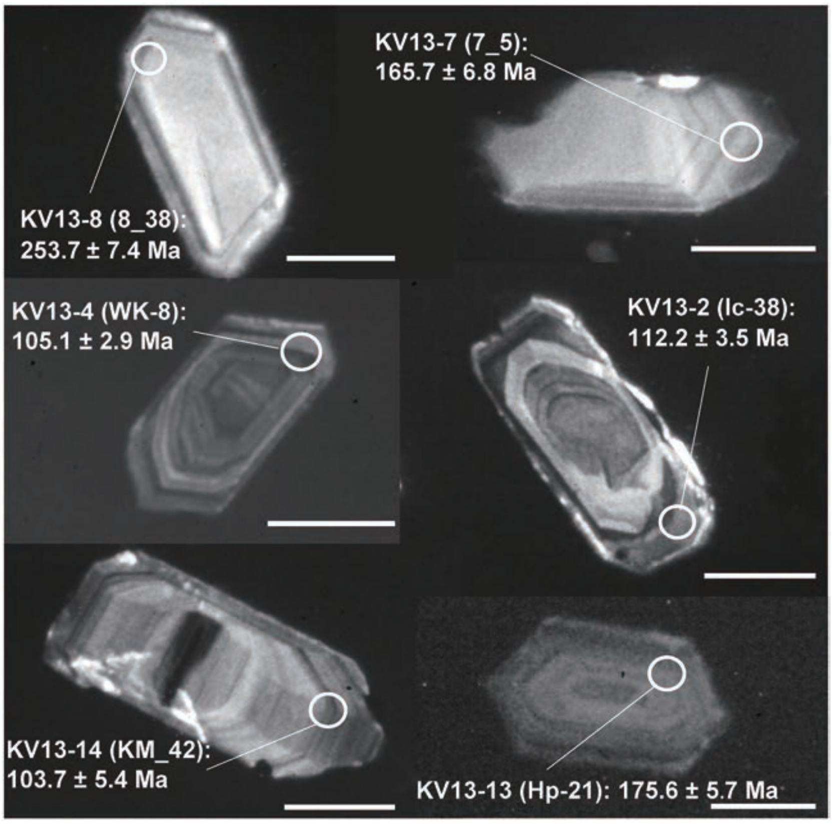

Fig. 2 Representative CL images of the analyzed zircons. The U-Pb ages are shown for each LA-ICP-MS analysis spot. The spot size is approximately 15 μm. Scale bar = 50 μm.

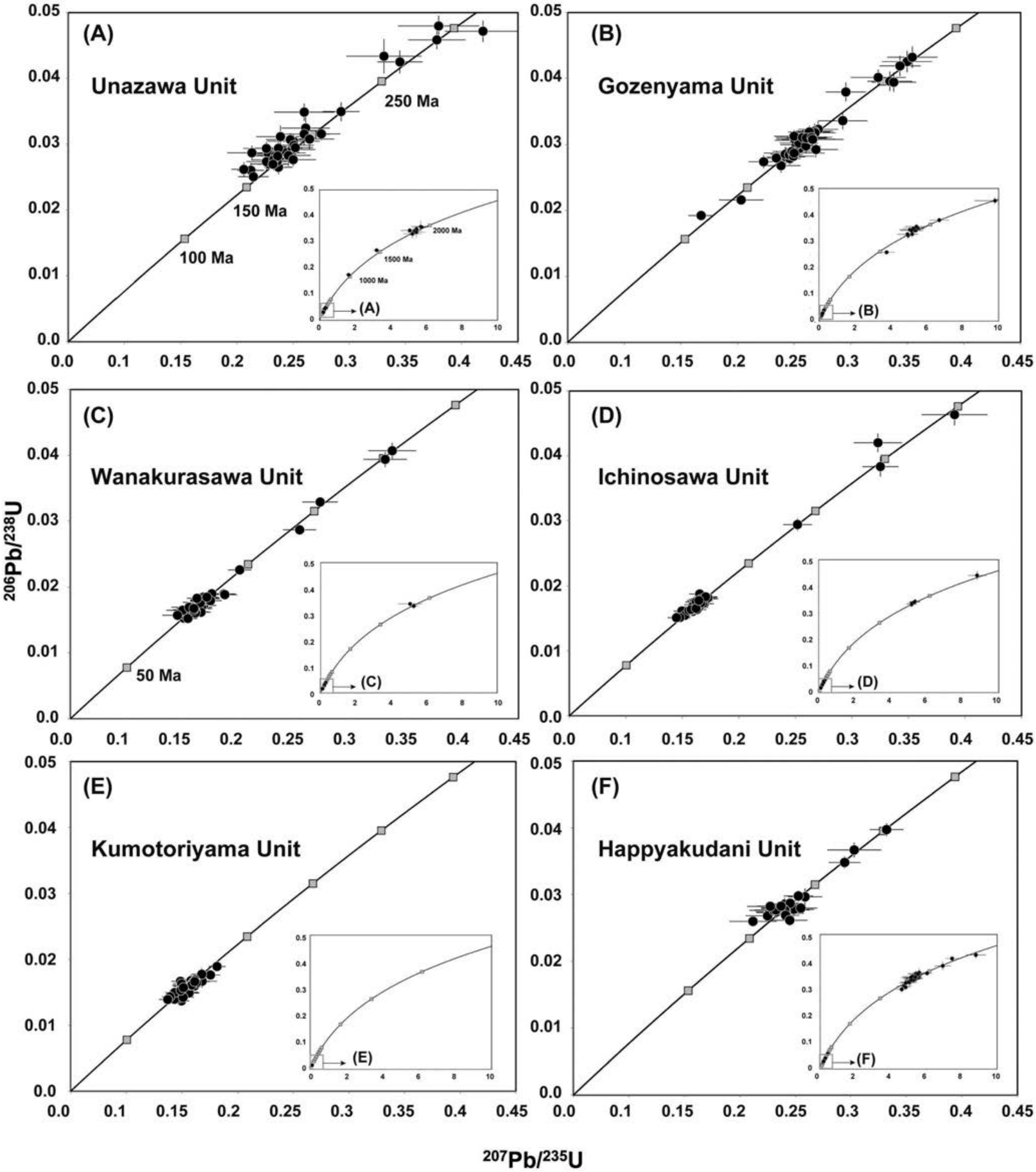

Fig. 3　U-Pb Concordia diagram for detrital zircons from sandstones in the Unazawa Unit (A), the Gozenyama Unit (B), the Wanakurasawa Unit (C), the Ichinosawa Unit (D), the Kumotoriyama Unit (E), and the Happyakudani Unit (F).

(1) Early-Late Jurassic - ca. 200-160 Ma (29 grains), (2) Permian-Triassic - ca. 300-220 Ma (6 grains) and (3) Proterozoic ages older than 1030 Ma (11 grains) (Figs. 3A and 4A, and Appendix Table 2). The youngest U-Pb age is 159.6 ± 4.9 Ma (Late Jurassic).

The Gozenyama Unit (KV13-8) has four distinct age clusters: (1) Early Cretaceous ages - 122.7 ± 3.8 and 137.6 ± 4.3 Ma (two grains), (2) Triassic-Jurassic - ca. 210-170 Ma (32 grains), (3) Permian ages - 270-240 Ma (7grains) and (4) Proterozoic ages older than 1480 Ma (15 grains) (Figs. 3B and 4B, and Appendix Table 3).

The youngest ages from the two units clearly demonstrate that their maximum deposition ages are Oxfordian and Aptian, which are largely consistent with paleontological data reported from siliceous shales in the same units in the Okutama area (e.g. Takashima and Koike, 1984; Takahashi, 2000). Moreover, the zircon age histograms of both units show that the proportion of detrital zircons with Proterozoic ages compared with the total number of grains is less than 25 %. This low proportion is the same as that of coeval sandstones in the Late Jurassic–Early Cretaceous AC in Shikoku, SW Japan (Sanbosan AC; Aoki *et al.*, 2012).

4.2. Ogochi Group

Most U–Pb data from sandstones in the Wanakurasawa (KV13-4), Ichinosawa (KV13-2) and Kumotoriyama (KV13-14) units have a mid-early Late Cretaceous age range of ca. 120–90 Ma (Appendix Tables 4–6 and Figs. 3–4). The youngest ages of each sample are 97.5 ± 2.3, 96.7 ± 4.3, 87.7 ± 1.9 Ma, respectively; these

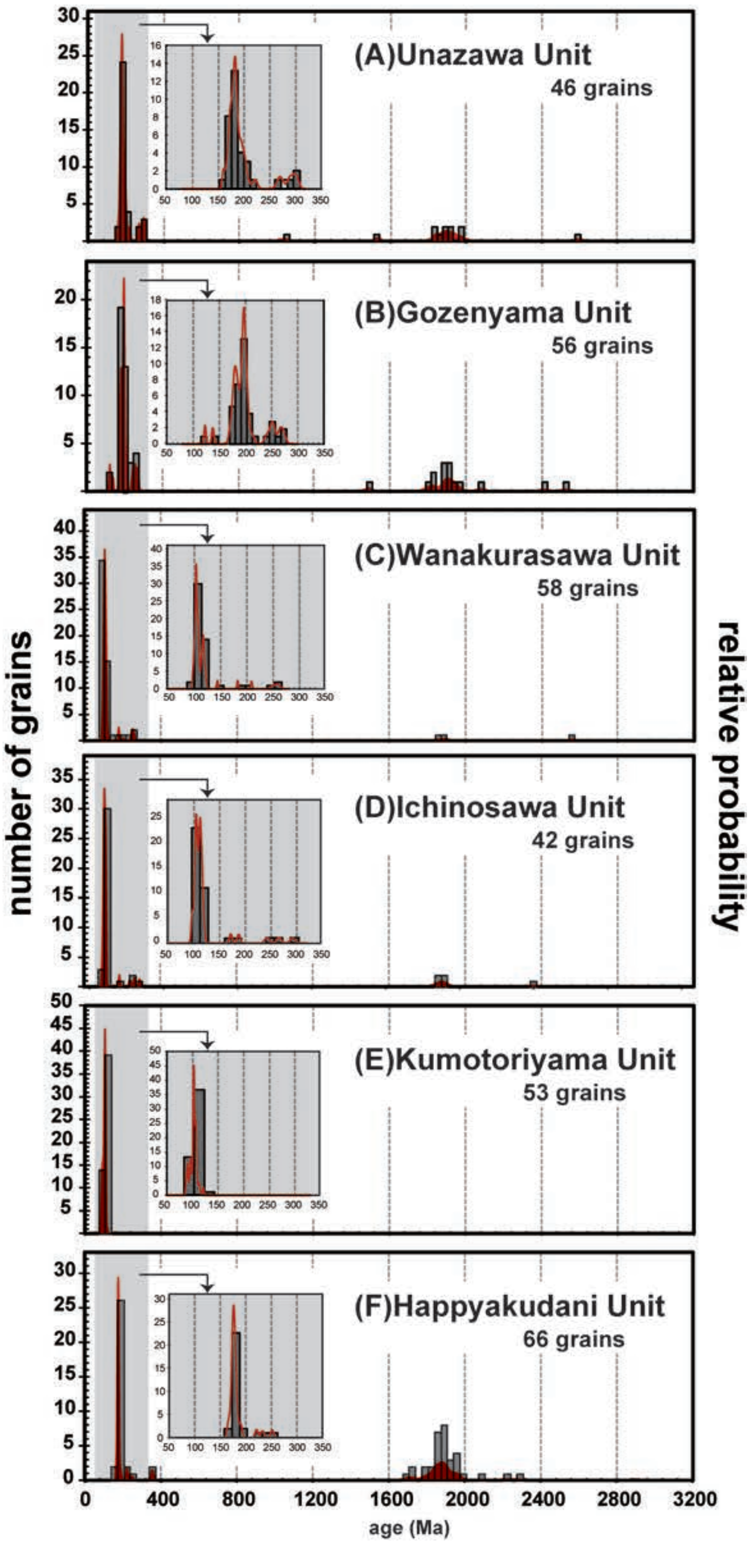

Figure. 4. Probability age frequency curves including histograms of detrital zircons from each unit.

are consistent with microfossil data from the equivalent units in the Okutama area (Iyota *et al.*, 1994). Also we confirm a small number of detrital zircons with Permian-Jurassic and Proterozoic ages; ca. 260-140 Ma (6 grains) and ca. 2560-1850 Ma (3 grains) from sandstones in the Wanakurasawa Unit, and ca. 300-170 Ma (5 grains) and 2350-1850 Ma (5 grains) in the Ichinosawa Unit, but we found no detrital zircons with those ages in the Kumotoriyama Unit.

The age histograms show that the Happyakudani Unit (KV13-13) has three age clusters: (1) Early-Middle Jurassic age - ca. 190-166 Ma (28 grains), (2) Permian-Triassic - ca. 360-220 Ma (5 grains) and (3) Proterozoic ages older than 1670 Ma (33 grains) (Appendix Table 7, and Figs. 3F and 4F). The youngest age is 165.5 ± 5.2 Ma (Middle Jurassic), which is significantly older than the microfossil age previously reported from the same unit in the Okutama area (Coniacian-Campanian; Iyota *et al.*, 1994).

5. Discussion

5.1. Constraints on time of deposition

The youngest zircon ages from terrigenous rocks can be used to constrain the maximum deposition age of their host rocks. The youngest zircon U-Pb ages for sandstones in the Unazawa and Gozenyama units (Jurassic AC), and Wanakurasawa, Ichinosawa and Kumotoriyama units (Cretaceous AC) are 159.6 ± 4.9, 122.7 ± 3.8, 97.5 ± 2.3, 96.7 ± 4.3 and 87.7 ± 1.9 Ma, respectively. As mentioned above, those ages are almost consistent with the deposition ages inferred from microfossil data reported from shales in the same units. The accretion polarity shown by the youngest age from each unit indicates tectonic-downward growth with time across the BTL. This is also consistent with the growth polarity previously estimated from biostratigraphic data from shales that make up the uppermost part of OPS. Hence, from this evidence we can say that the youngest zircon ages do indicate the time of deposition of each protolith near the oceanic plate convergent margin. Moreover, the tectonic-downward growth of the AC units with time is provided not only by the biostratigraphic ages from the shales, but also by the youngest zircon ages from sandstones in each AC unit.

Regarding the Happyakudani Unit, however, the youngest zircon age (165.5 ± 5.2 Ma; late Middle-early Late Jurassic) is significantly older than the previously reported microfossil age (Coniacian-Campanian; Iyota *et al.*, 1994). The age histogram shows that the population of Proterozoic detrital zircons is more than 50 % (Fig. 4). Sakai (1987) described the Jurassic sandstones in the Happyakudani Unit occur in allochthonous blocks. In addition, the age histogram of Happyakudani sample is quite similar to that of Middle Jurassic sandstones reported from other areas in Japan (e.g. Isozaki *et al.*, 2010; Fujisaki *et al.*, 2014). It follows that the Happyakudani sample used in this study is considered to be from an allochthonous sandstone block in the Middle Jurassic AC. Because Middle Jurassic sandstone blocks have not yet been reported from the Kumotoriyama Unit, it is suggested that the Middle Jurassic AC was widely exposed in the fore-arc region after the deposition of the Kumotoriyama Unit at 87.7 ± 1.9 Ma.

5.2. Role of arc batholith formation

Our new zircon U-Pb age data show the presence of many ca. 200-160 Ma and ca. 120-90 Ma detrital zircons in the Jurassic and Cretaceous sandstones, respectively (Fig. 4). Maruyama (1997) described that huge granitic arc batholiths formed in Jurassic and Cretaceous in the western Pacific-type orogen. It follows that detrital zircons in the ACs could be supplied from the arc batholiths widely exposed in the hinterland at that time. Thus, the largest cluster age gaps between the Jurassic and Cretaceous sandstones could reflect the shift of provenance probably by a change in topographic relief of the arc batholith formation in the Cretaceous.

The detrital zircon age data reported from sandstones in Late Jurassic-Cretaceous ACs (Aoki *et al.*, 2012; Saito *et al.*, 2014; this study) tend to contain relatively fewer zircons of Proterozoic age (< 30 % or nearly near-total absence) compered with Middle Jurassic sandstones in Japan (e.g. Isozaki *et al.*, 2010; Fujisaki *et al.*, 2014). This characteristic indicates a reduced supply of terrigenous clastics including Proterozoic zircons in the fore-arc from the Late Jurassic to Cretaceous. As to the provenance of the Proterozoic zircons in the Late Jurassic and Cretaceous AC units in Japan, two possible provenances have been considered; one is a Middle Jurassic AC and the other is the North-South China blocks (Isozaki *et al.*, 2010; Aoki *et al.*, 2012, 2014 and references therein). As discussed above, it is possible that the Middle Jurassic AC was widely exposed on the surface in the fore-arc region after 87.7 ± 1.9 Ma. Thus, the main provenance of the Proterozoic zircons was most likely the N-S China blocks.

Aoki *et al.* (2014) concentrated on the terrigenous supply system in the Cretaceous Pacific-type orogen in Japan and pointed out that Proterozoic zircons originating from the N-S China blocks were supplied in abundance to the back-arc side, but few reached the coeval fore-arc side, and that the change in topographic relief associated with arc batholith formation was critical in determining and controlling the supply routes of terrigenous clastics to the arc-related basins. Therefore, the difference in zircon populations between the Middle Jurassic and the Late Jurassic-Cretaceous sandstones would be due to the topological change in the fore-arc region. Probably, the high-standing batholith served as a barrier to restrict the supply route of the terrigenous clastics from the back-arc side where the N-S China cratons were widely exposed. In addition, the amount of Proterozoic zircons in the Middle Jurassic sandstone block (youngest zircon age: 165.5 ± 5.2 Ma) included in the Happyakudani Unit was significantly decreased compared with that in the other Middle Jurassic AC units (youngest ages: ca. 186-170 Ma; Fujisaki *et al*., 2014). Hence, the beginning of role of arc batholith as a major control of the terrigenous supply routes in the Late Jurassic-Cretaceous Japan is considered to be at ca. 170-160 Ma.

Acknowledgements

We thank Brian F. Windley for grammatical improvements. Constructive comments by Tetsumaru Itaya and Tatsuki Tsujimori are quite helpful in revision. We are also grateful to Chitaro Gouzu and Koshi Yagi for this opportunity for publication.

References

Aoki, K., Isozaki, Y., Kofukuda, D., Sato, T., Yamamoto, A., Maki, K., Sakata, S. and Hirata, T. (2014) Provenance diversification within an arc-trench system induced by batholith development: the Cretaceous Japan case. *Terra Nova*, **26**, 139-149.

Aoki, K., Isozaki, Y., Yamamoto, S., Maki, K., Yokoyama, T. and Hirata, T. (2012) Tectonic erosion in a Pacific-type orogen: Cretaceous tectonics in Japan. *Geology*, **40**, 1087-1090.

Chew, D.M., Petrus, J. A., Kamber, B. S. (2014) U-Pb LA-ICPMS dating using accessory mineral standards with variable common Pb. *Chemical Geology*, **363**, 185-199.

Chichibu Geologic Research Group (1966) Geology in the Vicinity of the Tokyo University Forest at Chichibu. Miscellaneous Information, Tokyo University Forest, **16**, 73-85 (in Japanese with English abstract).

Clift, P. D., Carter, A., Draut, A. E., Long, H. V., Chew, D. M., and Schouten, H. A. (2009) Detrital U-Pb zircon dating of lower Ordovician syn-arc-continent collision conglomerates in the Irish Caledonides. *Tectonophysics*, **479**, 165-174.

Corfu, F., Hanchar, J. M., Hoskin P.W.O., and Kinny, P. (2003) Atlas of zircon textures. In: Zircon (eds. Hanchar, J. M. and Hoskin P. W. O.), Reviews in Mineralogy and Geochemistry, Mineralogical Society of America and Geochemical Society, **53**. 469-500.

Dickinson, W.R., and Gehrels, G.E. (2008) U-Pb ages of detrital zircons in relation to paleogeography: Triassic paleodrainage networks and sediment dispersal across southwest Laurentia. *Journal of Sedimentary Research*, **78**, 745-764.

Eggins, S. M., Kinsley, L. P. J., Shelley, J. M. G. (1998) Deposition and element fractionation processes during atmospheric pressure laser sampling for analysis by ICP-MS. *Applied Surface Science*, **129**, 278-286.

Fujimoto, H., Kawata, K., Miyazawa, S., Morikawa, R., Arai, F., Takano, T., Yoshida, S., Hara, K., Tazuke, H. and Madoo, H. (1950) Geological studies of the Oku-chichibu. *Bulletin of the Chichibu Museum of Natural History*, **1**, 1-28 (in Japanese with English abstract).

Fujisaki, W., Isozaki, Y., Maki, K., Sakata, S., Hirata, T., Maruyama, S. (2014) Age spectra of detrital zircon of the Jurassic clastic rocks of the Mino-Tanba AC belt in SW Japan: constraints to the provenance of the mid-Mesozoic trench in East Asia. *Journal of Asian Earth Science*, **88**, 62-73.

Gradstein, F. M., Ogg, G., Schmitz, M., Ogg, G. M. (2012) The Geologic Time Scale 2012. Elsevier, 1144p., Amsterdam.

Günther, D. Heinrich, C. A. (1999) Enhanced sensitivity in laser ablation-ICP mass spectrometry using helium-argon mixtures as aerosol carrier. *Journal of Analytical Atomic Spectrometry*, **14**, 1363-1368.

Hara, H and Hisada, K. (2005) Metamorphic age of the Southern Chichibu and Shimanto accretionary complexes in the Mitsumine district of the Kanto Mountains, central Japan: K-Ar ages of illite from phylite. *The Journal of Geological Society of Japan*, **111**, 217-223 (in Japanese with English abstract).

Hara, H and Hisada, K. (2007) Tectono-metamorphic evolution of the Cretaceous Shimanto accretionary complex, central Japan: Constraints from fluid inclusion analysis of syn-tectonic veins. *Island Arc*, **16**, 57-68.

Hara, H., Hisada, K., and Kimura, K. (1998) Paleo-geothermal structure based on illite crystallinity of the Chichibu and Shimanto Belts in the Kanto Mountains, central Japan. *The Journal of Geological Society of Japan*, **104**, 705-717 (in Japanese with English abstract).

Hara, H., Ueno, H., Tsunoda, K., Hisada, K., Shimizu, M., Takeuchi, K. and Ozaki, M. (2010) Geology of the Mitsumine district. Quadrangle series, 1:50,000, Geologic Survey of Japan, AIST, 110p (in Japanese with English abstract).

Hisada, K. (1984) Geology of the Paleozoic and Mesozoic strata in the Ashigakubo-Kamazawa area, sothern Kanto Mountains. *The Journal of Geological Soceity of Japan*, **90**, 139-156 (in Japanese with English abstract).

Iizuka, T., Hirata, T. (2004) Simultaneous determinations of U-Pb age and REE abundances for zircons using ArF excimer laser ablation-ICPMS. *Geochemical Journal*, **38**, 229-241.

Isozaki, Y. (1996) Anatomy and genesis of a subduction-related orogen: A new view of geotectonic subdivision and evolution of the Japanese Islands. *The Island Arc*, **5**, 289-320.

Isozaki, Y. (1997) Jurassic accretion tectonics of Japan. *Island Arc*, **6**, 25-51.

Isozaki, Y and Nishimura, Y. (1989) Fusaki Formation, Jurassic subduction-accretion complex on Ishigaki Island, southern Ryukyus and its geologic implication to Late Mesozoic convergent margin of East Asia. *Memoirs of the Geological Society of Japan*, **33**, 259-275 (in Japanese with English abstract).

Isozaki, Y., Aoki, K., Nakama, T., Yanai, S. (2010) New insight into a subduction-related orogen: Reappraisal on geotectonic framework and evolution of the Japanese Islands. *Gondwana Research*, **18**, 82-105.

Isozaki, Y., Aoki, K., Sakata, S., Hirata, T. (2014) The eastern extension of Paleozoic South China in NE Japan evidenced by detrital zircon. *GFF*, **136**, 116-119.

Iyota, N., Hisada, K. and Sashida, K. (1994) The Ogochi Group of the Shimanto Terrane in the Kanto Mountains, central Japan. Science reports of the Institute of Geoscience, University of Tsukuba. *Section B, Geological sciences*, **15**, 47-69.

Jackson, S. E., Pearson, N. J., Griffin, W. L., Belousova, E. A. (2004) The application of laser ablation-inductively coupled plasma-mass spectrometry 561 to in situ U-Pb zircon geochronology. *Chemical Geology*, **211**, 47-69.

Jaffey, A. H., Flynn, K. F., Glendenin, L. E., Bentleyt, W. C., and Essling, A. M. (1971) Precision measurement of half-lives and specific activities of ^{235}U and ^{238}U. *Physical Review C*, **4**, 1889-1906.

Kimura, G. (1997) Cretaceous episodic growth of the Japanese Islands. *The Island Arc*, **6**, 52-68.

Kusky, T. M., Windley, B. F., Safonova, I., Wakita, K., Wakabashi, J., Polat, A., and Santosh, M. (2013) Recognition of ocean plate stratigraphy in accretionary orogens through Earth history: a record of 3.8 billion years of sea floor spreading, subduction, and accretion. *Gondwana Research*, **24**, 501-547.

LaMaskin, T.A. (2012) Detrital zircon facies of Cordilleran terranes in western North America. *GSA Today*, **22**, 4-11.

Ludwig, K. (2003) Isoplot 3.0. Special Publication, v. 4, Berkeley Geochronology Center.

Maruyama, S. (1997) Pacific-type orogeny revisited: Miyashiro-type orogeny proposed. *The Island Arc*, **6**, 91-120.

Matsuda, T., and Isozaki, Y. (1991) Well-documented travel history of Mesozoic pelagic cherts in Japan: from remote ocean to subduction zone. *Tectonics*, **10**, 475-499.

Matsuoka, A., Yamakita, S., Sakakibara, M. and Hisada, K. (1998) Unit division for the Chichibu composite belt from view point of accretionary tectonics and geology of western Shikoku, Japan. *The Journal of Geological Society of Japan*, **104**, 634-653 (in Japanese with English abstract).

Okawa, H., Shimojo, M., Orihashi, Y., Yamamoto, K., Hirata, T., Sano, S., Ishizaki, Y., Kouchi, Y., Yanai, S. and Otoh, S. (2013) Detrital zircon geochronology of the Silurian-Lower Cretaceous continuous succession of the South Kitakami Belt, Northeast Japan. *Memoir of the Fukui Prefectural Dinosaur Museum*, **12**, 35-78.

Paton, C., Hellstrom, J., Paul, B., Woodhead, J. and Hergt, J. (2011) Iolite: Freeware for the visualisation and processing of mass spectrometric data. *Journal of Analytical Atomic Spectrometry*. **26**, 2508-2518.

Saito, T., Okada, Y., Fujisaki, W., Sawaki, Y., Sakata, S., Dohm, J., Maruyama, S. and Hirata, T. (2014) Accreted Kula plate fragment at 94Ma in the Yokonami-melange, Shimanto belt, Shikoku, Japan. *Tectonophysics*, **623**, 136-146.

Sakai, A. (1987) Geology of the Itsukaichi district. Quadrangle Series, 1:50,000, Geologic Survey of Japan, AIST, 75p (in Japanese with English abstract).

Schmitz, M. D., Bowring, S. A., Ireland, T. R. (2003) Evaluation of Duluth Complexanorthositic series (AS3) zircon as a U-Pb geochronological standard: New high-precision isotope dilution thermal ionization mass spectrometry results. *Geochimica et Cosmochimica Acta*, **67**, 3665-3672.

Sláma, J., Košler, J., Condon, D. J., Crowley, J. L., Gerdes, A., Hancharg, J. M., Horstwood, M. S. A., Morris, G., A., Nasdala, L., Norberg, N., Schaltegger, U., Schoene, B., Tubrett, M. N., Whitehouse, M. J. (2008) Plesovice zircon - A new natural reference material for U-Pb and Hf isotopic microanalysis. *Chemical Geology*, **249**, 1-35.

Stern, R. A. (1997) "The GSC Sensitive High Resolution Ion Microprobe (SHRIMP): analytical techniques of zircon U-Th-Pb age determinations and performance evaluation." Radiogenic age and isotope studies. Report 10.

Storey, C. D., Jeffries, T. E., Smith, M. (2006) Common lead-corrected laser ablation ICP-MS U-Pb systematics and geochronology of titanite. *Chemical Geology*, **227**, 37-52.

Taira, A., Katto, J., Tashiro, M., Okumura, M. and Kodama, K. (1988) The Shimanto Belt in Shikoku, Japan-evolution of Cretaceous to Miocene accretionary prism. *Modern Geology*, **12**, 5-46.

Takahashi, O. (2000) Tectonostratigraphic study of the Chichibu and Shimanto belts in the Kanto Mountains, central Japan. *The Journal of Geological Society of Japan*, **106**, 836-852.

Takashima, K., and Koike, T. (1984) Stratigraphy and geological structure of the Mesozoic strata in the Gozenyama Itsukaichi area, southeastern part of the Kanto Mountains. *Science Report of the Yokohama National University*, sec, **2**, 29-49.

Tunheng, A. and Hirata, T. (2004) Development of signal smoothing 715 device for precise elemental analysis using laser ablation-ICP-mass spectrometry. *Journal of Analytical Atomic Spectrometry*, **19**, 932-934.

Wiedenbeck, M., Alle, P., Corfu, F., Griffin, W. L., Meier, M., Oberli, F., Von Quadt, A., Roddick, J. C., Spiegel, W. (1995) Three natural zircon standards for U-Th-Pb, Lu-Hf, trace element and REE analyses. *Geostandards Newsletter*, **19**, 1-23.

Wiedenbeck, M., Hanchar, J. M., Peck, W. H., Sylvester, P., Valley, J., Whitehouse, M., Kronz, A., Morishita, Y., Nasdala, L., Fiebig, J., Franchi, I., Girard, J.-P., Greenwood, R. C., Hinton, R., Kita, N., Mason, P. R. D., Norman, M., Ogasawara, M., Piccoli, P. M., Rhede, D., Satoh, H., Schulz-Dobrick, B., Skår, O., Spicuzza, M. J., Terada, K., Tindle, A., Togashi, S., Vennemann, T., Xie, Q., Zheng, Y. F. (2004) Further characterisation of the 91500 zircon crystal. *Geostandards and Geoanalytical Research*, **28**, 9-39.

地質技術　第5号（蒜山地質年代学研究所創立20周年記念特集），11-27頁（2015）

関東山地に産するジュラ紀－白亜紀付加体砂岩の砕屑性ジルコン年代：陸弧後背地の変遷

青木 一勝[1)]・磯崎 行雄[2)]・坂田 周平[3)]・佐藤 友彦[4)]・山本 伸次[2)]・平田 岳史[3)]

[1)] 岡山理科大学理学部基礎理学科，〒700-0005　岡山市北区理大町1-1
[2)] 東京大学大学院総合文化研究科宇宙地球科学教室，〒153-8902　東京都目黒区駒場3-8-1
[3)] 京都大学大学院理学研究科地質学鉱物学教室，〒606-8502　京都市左京区北白川追分町
[4)] 東京工業大学地球生命研究所，〒152-8551　東京都目黒区大岡山2-12-1

日本語要旨　付加体の主体をなす粗粒砕屑岩の後背地情報を得るために，関東山地三峰地域に産する秩父帯ジュラ紀付加体および四万十帯北帯白亜紀付加体の6つのユニットの砂岩から砕屑性ジルコンを分離し，LA-ICP-MSを用いてU-Pb年代測定を行った．各ユニットの最も若いジルコン年代は，頁岩産の放散虫年代と一致し，仏像構造線を挟んで，6つの付加体ユニットが構造的下位に向かって断続的に成長したことが確認された．ジュラ紀および白亜紀付加体の砂岩中には各々約200-160 Ma，約120-90 Maのジルコン粒子が卓越し，付加体形成時の陸縁に，直前に形成された弧花崗岩（バソリス）帯が広域に露出していたことを示す．一方，大陸由来の先カンブリア時代ジルコンの年代頻度は経年変化し，ジュラ紀末～白亜紀後期の花崗岩バソリスの形成・上昇・削剥は，大陸内部から当時の前弧域／海溝への砕屑物の供給経路に大きく影響したと推定される．

対訳　Mitsumine 三峰，Urayama 浦山，Ogochi 小河内，Unazawa 海沢，Gozenyama 御前山，Wanakurasawa 和名倉沢，Ichinosawa 市ノ沢，Kumotoriyama 雲取山，Happyakudani 八百谷

Appendix A

In situ zircon U-Pb dating was carried out using a Nu AttoM single-collector ICP-MS (Nu instruments, Wrexham, UK) coupled to a NWR-193 laser-ablation system (ESI, Portland, US) that utilizes a 193 nm ArF excimer laser at the Department of Geology and Mineralogy, Kyoto University. The laser was operated with an output energy of ～ 9 mJ per pulse, repetition rate of 8 Hz and laser spot size diameter of 15 μm, providing an estimated power density of the sample of < 2.5 Jcm^{-2}. The total count of the laser pulse during ablation was 180 shots. The ablation occurred in helium gas within a sample cell of < 1ml, and then the ablated sample aerosol and helium gas were mixed with argon gas downstream of the cell. The helium minimizes redeposition of ejecta or condensates, while argon provides efficient sample transport to the ICP-MS (Eggins *et al.*, 1998; Günther and Heinrich, 1999; Jackson *et al.*, 2004). A baffled-type stabilizer (volume: 52 ml) was used (Tunheng and Hirata, 2004), and to reduce the isobaric interference, an Hg-trap device with an activated charcoal filter was applied to the Ar make-up gas before mixing with He carrier gas (Hirata *et al.*, 2005). Prior to each individual analysis, regions of interest were pre-ablated using a few pulses of the laser with a laser spot size diameter of 20 or 30 μm in order to remove potential surface contamination, dramatically reducing common Pb contamination (Iizuka and Hirata, 2004).

The ICP-MS was optimized using continuous ablation of a 91500 zircon standard (Wiedenbeck *et al.* 1995, 2004), a NIST SRM 610 to provide maximum sensitivity while maintaining low oxide formation ($^{232}Th^{16}O^+/^{232}Th$ < 1%). Data were acquired for six isotopes, ^{202}Hg, ^{204}Pb, ^{206}Pb, ^{207}Pb, ^{232}Th and ^{238}U when measuring the signal intensity at the peak maximum. For the analysis with a Nu AttoM with NWR-193 excimer laser, the ages and isotope ratios of zircon samples were calculated using an in-house excel spread sheet. Gas blank and ablation data for each analysis were collected over ～80 and ～8 seconds, respectively. Data were acquired for multiple groups of 10 unknowns sample-bracketed by quartets of analyses of the 91500 zircon standard (Wiedenbeck *et al.*, 1995, 2004) following a single background analysis.

Through all the analyses, ^{202}Hg was monitored to correct the isobaric interference of ^{204}Hg on ^{204}Pb. Zircon ages can be corrected for common Pb contamination based on measurement of ^{204}Pb (e.g. Stern, 1997; Storey *et al.*, 2006; Chew *et al.*, 2014). In this study, due to the very low ^{204}Pb counts, it was not possible to apply the common Pb correction with sufficient precision. Therefore, we rejected those data, which showed a significant level of contribution from common Pb ($(^{206}Pb/^{204}Pb)_{total}$ < 1000, $(^{207}Pb/^{204}Pb)_{total}$ < 100), and no common Pb correction was made.

All uncertainties are quoted at a 2 sigma level to which repeatability of measurements of primary standard is propagated based on quadratic addition. ^{235}U was calculated from ^{238}U using a $^{238}U/^{235}U$ ratio of 137.88 (Jaffey *et al.*, 1971). Through all the analyses, Plešovice (337.13 ± 0.37 Ma, Sláma *et al.*, 2008) and AS-3 (1099.1 ± 0.2 Ma, Schmitz *et al.*, 2003) zircons were measured as secondary standards for quality control. The summary of instrumental settings and the resulting ages of secondary zircons are shown in the Appendix Table 1.

Appendix Table 1 Summary of instrumental settings and the resulting ages of secondary zircons.

Laser ablation system for ArF excimer laser	
Ablation cell	Two volume cell
Wavelength	193 nm
Pulse energy	9.0 mJ
Pulse width	4-6 ns
Energy density/ Fulence	< 2.5 Jcm^{-2}
Repetition rate	8 Hz
Spot diameter	15 μm
Sampling mode/pattern	Single hole drilling, 1 cleaning pulse
Carrier gas and flow	He, 0.650 l min^{-1}
Effective cell volume	< 1ml
Ablation duration	22.5 sec
ICP-MS instrument for Nu AttoM single collector ICP-MS	
Sample introduction	Ablation aerosol only, using in-house signal smoothing device (Tunheng and Hirata, 2004)
RF power	1300 W
Cooling gas flow rate	13
Auxiliary gas flow rate	0.9
Make-up gas flow	0.90 l min^{-1}
Detection system	mixed attenuation-multiple ion counting
Masses measured	202, 204, 206, 207, 232, 238 amu
Integration time per peak	50 ms (masses 202, 204, 232), 150 ms (masse 206), 200 ms (masse 207), 100 ms (mass 238)
Total integration time per reading	0.678
IC dead time	12.2 ns
Typical oxide rate (ThO/O)	0.7%
Data processing	
Gas blank	10 seconds prior to each ablation spot
Calibration strategy	91500 used as primary reference material, Plesovice and AS-3 used as secondaries for quality control
Reference material information	91500 $^{206}Pb/^{238}U$: 0.1792, $^{207}Pb/^{206}Pb$: 0.0749 (Wiedenbeck et al. 1995)
Data reduction	Time resolved analysis. We skipped first signals at a few seconds for waiting stabilization, and next signals for about 20 seconds were used for calculation.
Mass discrimination	Mass bias correction for all ratios normalized to the primary reference material
Common Pb correction	No common Pb correction applied.
Uncertainty level & propagation	Ages are quoted at 2 SE absolute, propagation is by quadratic addition. Repeatability of reference material uncertainty was applied (Paton et al., 2011).
Quality control/validation	Plesovice: Wtd ave. $^{206}Pb/^{238}U$ age = 340.6 ± 6.7 (MSWD = 1.6, n = 5), $^{207}Pb/^{235}U$ age = 336.7 ± 7.2 (MSWD = 0.64, n = 5), AS-3: Wtd ave. $^{206}Pb/^{238}U$ age = 1108 ± 14 (MSWD = 0.14, n = 10), $^{207}Pb/^{235}U$ age = 1094 ± 13 (MSWD = 0.38, n = 10) all errors are quoted at 95% confidence.

Appendix Table 2 LA-ICP-MS U-Pb isotopic analytical data for separated zircons from the Unazawa Unit (sample KV13-7).

Grain number	$^{206}Pb/^{238}U$			$^{207}Pb/^{235}U$			$^{207}Pb/^{206}Pb$			Age					
										$^{206}Pb/^{238}U$			$^{207}Pb/^{235}U$		
7_1	0.0265	±	0.00108	0.1869	±	0.01245	0.0512	±	0.00270	168.6	±	6.8	174.0	±	10.7
7_2	0.0287	±	0.00115	0.1986	±	0.01248	0.0502	±	0.00243	182.3	±	7.2	183.9	±	10.6
7_3	0.0281	±	0.00114	0.1880	±	0.01228	0.0485	±	0.00249	178.6	±	7.1	174.9	±	10.6
7_4	0.0425	±	0.00173	0.2950	±	0.01991	0.0503	±	0.00271	268.3	±	10.7	262.5	±	15.7
7_5	0.0260	±	0.00108	0.1623	±	0.01176	0.0452	±	0.00269	165.7	±	6.8	152.7	±	10.3
7_6	0.0288	±	0.00119	0.1915	±	0.01387	0.0483	±	0.00287	182.8	±	7.5	177.9	±	11.9
7_7	0.0284	±	0.00118	0.1814	±	0.01352	0.0463	±	0.00286	180.5	±	7.4	169.2	±	11.7
7_8	0.0349	±	0.00142	0.2427	±	0.01627	0.0504	±	0.00268	221.4	±	8.9	220.6	±	13.4
7_11	0.3395	±	0.00702	5.3300	±	0.22738	0.1139	±	0.00425	1884.3	±	33.9	1873.7	±	37.1
7_12	0.3491	±	0.00742	5.4490	±	0.23981	0.1132	±	0.00436	1930.2	±	35.6	1892.6	±	38.5
7_13	0.0290	±	0.00065	0.1917	±	0.01015	0.0479	±	0.00230	184.4	±	4.1	178.1	±	8.7
7_14	0.0287	±	0.00063	0.1938	±	0.00973	0.0489	±	0.00221	182.6	±	3.9	179.9	±	8.3
7_15	0.3305	±	0.00683	5.2282	±	0.22264	0.1147	±	0.00427	1840.6	±	33.2	1857.2	±	37.0
7_16	0.0459	±	0.00139	0.3279	±	0.02540	0.0519	±	0.00370	289.0	±	8.6	288.0	±	19.6
7_17	0.0270	±	0.00088	0.1785	±	0.01595	0.0480	±	0.00399	171.6	±	5.6	166.8	±	13.8
7_18	0.0251	±	0.00077	0.1646	±	0.01335	0.0476	±	0.00357	159.6	±	4.9	154.8	±	11.7
7_19	0.0472	±	0.00161	0.3689	±	0.03382	0.0567	±	0.00483	297.1	±	9.9	318.8	±	25.4
7_20	0.4951	±	0.01399	13.0130	±	0.88332	0.1906	±	0.01177	2592.6	±	60.6	2680.6	±	66.1
7_21	0.0286	±	0.00096	0.1778	±	0.01661	0.0451	±	0.00393	181.7	±	6.0	166.2	±	14.4
7_22	0.0292	±	0.00105	0.1992	±	0.02029	0.0495	±	0.00472	185.6	±	6.6	184.5	±	17.3
7_23	0.0274	±	0.00079	0.1858	±	0.01337	0.0491	±	0.00324	174.4	±	5.0	173.1	±	11.5
7_24	0.0282	±	0.00082	0.1842	±	0.01838	0.0473	±	0.00452	179.4	±	5.1	171.6	±	15.9
7_25	0.0304	±	0.00103	0.2003	±	0.02314	0.0477	±	0.00527	193.4	±	6.4	185.4	±	19.8
7_26	0.3442	±	0.00961	5.0653	±	0.48186	0.1067	±	0.00971	1906.9	±	46.3	1830.3	±	84.1
7_28	0.0480	±	0.00155	0.3294	±	0.03615	0.0498	±	0.00522	302.0	±	9.5	289.1	±	28.0
7_31	0.0307	±	0.00097	0.1975	±	0.02145	0.0467	±	0.00485	194.9	±	6.1	183.0	±	18.4
7_32	0.0294	±	0.00173	0.1869	±	0.02115	0.0461	±	0.00446	186.7	±	10.9	174.0	±	18.3
7_33	0.0274	±	0.00156	0.1763	±	0.01772	0.0467	±	0.00387	174.0	±	9.8	164.8	±	15.4
7_34	0.0276	±	0.00161	0.1827	±	0.01986	0.0479	±	0.00440	175.8	±	10.1	170.3	±	17.2
7_35	0.0283	±	0.00161	0.1958	±	0.01959	0.0502	±	0.00412	179.9	±	10.1	181.6	±	16.8
7_36	0.3375	±	0.01894	5.4355	±	0.49869	0.1168	±	0.00848	1874.5	±	91.9	1890.5	±	81.9
7_37	0.3589	±	0.02009	5.6855	±	0.51884	0.1149	±	0.00828	1977.2	±	96.0	1929.2	±	82.0
7_38	0.0434	±	0.00260	0.2808	±	0.03343	0.0470	±	0.00483	273.7	±	16.1	251.3	±	26.9
7_39	0.0282	±	0.00090	0.1862	±	0.01582	0.0479	±	0.00377	179.3	±	5.6	173.4	±	13.6
7_40	0.0298	±	0.00096	0.2009	±	0.01725	0.0488	±	0.00389	189.6	±	6.0	185.9	±	14.7
7_41	0.0270	±	0.00079	0.1820	±	0.01314	0.0490	±	0.00323	171.5	±	5.0	169.8	±	11.4
7_42	0.2683	±	0.00763	3.2056	±	0.20706	0.0867	±	0.00503	1532.2	±	38.9	1458.5	±	51.3
7_43	0.0316	±	0.00094	0.2252	±	0.01677	0.0517	±	0.00353	200.5	±	5.9	206.2	±	14.0
7_44	0.0277	±	0.00100	0.2000	±	0.02012	0.0525	±	0.00492	175.9	±	6.3	185.2	±	17.2
7_45	0.0295	±	0.00089	0.2020	±	0.01559	0.0497	±	0.00353	187.3	±	5.6	186.8	±	13.3
7_46	0.3572	±	0.00976	5.7300	±	0.34904	0.1163	±	0.00633	1968.8	±	46.5	1935.9	±	54.1
7_47	0.0325	±	0.00165	0.2112	±	0.02132	0.0472	±	0.00411	205.9	±	10.3	194.5	±	18.0
7_48	0.1744	±	0.00883	1.6329	±	0.16084	0.0679	±	0.00574	1036.5	±	48.7	983.0	±	64.0
7_49	0.0315	±	0.00165	0.2098	±	0.02276	0.0482	±	0.00459	200.2	±	10.3	193.4	±	19.3
7_50	0.3311	±	0.01675	5.2153	±	0.51053	0.1143	±	0.00957	1843.6	±	81.6	1855.1	±	87.0
7_52	0.0308	±	0.00157	0.2146	±	0.02176	0.0506	±	0.00443	195.4	±	9.8	197.4	±	18.4

All errors are quoted at 2σ.

Appendix Table 3 LA-ICP-MS U-Pb isotopic analytical data for separated zircons from the Gozenyama Unit (sample KV13-8).

Grain number	$^{206}Pb/^{238}U$	$^{207}Pb/^{235}U$	$^{207}Pb/^{206}Pb$	Age	
				$^{206}Pb/^{238}U$	$^{207}Pb/^{235}U$
8_1	0.0274 ± 0.00097	0.1731 ± 0.01326	0.0458 ± 0.00311	174.1 ± 6.1	162.1 ± 11.5
8_2	0.0268 ± 0.00103	0.1884 ± 0.01691	0.0510 ± 0.00414	170.4 ± 6.4	175.3 ± 14.5
8_3	0.0306 ± 0.00120	0.2020 ± 0.01913	0.0478 ± 0.00413	194.4 ± 7.5	186.8 ± 16.3
8_4	0.0336 ± 0.00129	0.2429 ± 0.02172	0.0524 ± 0.00424	213.0 ± 8.0	220.8 ± 17.9
8_5	0.0281 ± 0.00106	0.1928 ± 0.01694	0.0498 ± 0.00394	178.7 ± 6.7	179.0 ± 14.5
8_6	0.0311 ± 0.00113	0.2121 ± 0.01689	0.0494 ± 0.00351	197.5 ± 7.1	195.3 ± 14.2
8_7	0.0323 ± 0.00117	0.2212 ± 0.01756	0.0497 ± 0.00351	205.0 ± 7.3	202.9 ± 14.7
8_8	0.0320 ± 0.00113	0.2179 ± 0.01640	0.0494 ± 0.00328	203.1 ± 7.1	200.1 ± 13.8
8_10	0.0317 ± 0.00133	0.1997 ± 0.01965	0.0458 ± 0.00407	200.9 ± 8.3	184.9 ± 16.8
8_12	0.0425 ± 0.00160	0.2998 ± 0.02188	0.0511 ± 0.00319	268.6 ± 9.9	266.2 ± 17.2
8_13	0.0432 ± 0.00163	0.3044 ± 0.02213	0.0511 ± 0.00318	272.7 ± 10.1	269.8 ± 17.4
8_15	0.0396 ± 0.00147	0.2846 ± 0.01976	0.0522 ± 0.00306	250.2 ± 9.1	254.3 ± 15.7
8_16	0.3278 ± 0.01203	5.1879 ± 0.33549	0.1148 ± 0.00611	1827.8 ± 58.7	1850.6 ± 56.6
8_17	0.0279 ± 0.00104	0.1843 ± 0.01315	0.0478 ± 0.00291	177.6 ± 6.5	171.7 ± 11.3
8_18	0.0379 ± 0.00142	0.2456 ± 0.01758	0.0470 ± 0.00287	240.0 ± 8.8	223.0 ± 14.4
8_19	0.4795 ± 0.01536	10.7278 ± 0.38965	0.1623 ± 0.00278	2525.2 ± 67.3	2499.8 ± 34.3
8_20	0.0294 ± 0.00103	0.2045 ± 0.01233	0.0505 ± 0.00248	186.6 ± 6.4	189.0 ± 10.5
8_21	0.0300 ± 0.00108	0.2017 ± 0.01386	0.0488 ± 0.00285	190.3 ± 6.8	186.5 ± 11.8
8_22	0.0310 ± 0.00108	0.2155 ± 0.01270	0.0505 ± 0.00240	196.5 ± 6.7	198.1 ± 10.7
8_23	0.0394 ± 0.00143	0.2880 ± 0.01965	0.0530 ± 0.00306	249.2 ± 8.9	257.0 ± 15.6
8_24	0.0279 ± 0.00092	0.1963 ± 0.00920	0.0511 ± 0.00170	177.1 ± 5.8	182.0 ± 7.8
8_25	0.0308 ± 0.00121	0.2004 ± 0.01599	0.0472 ± 0.00328	195.6 ± 7.5	185.5 ± 13.6
8_26	0.0419 ± 0.00152	0.2934 ± 0.01803	0.0508 ± 0.00252	264.5 ± 9.4	261.3 ± 14.3
8_27	0.0302 ± 0.00120	0.2042 ± 0.01678	0.0490 ± 0.00353	191.9 ± 7.5	188.7 ± 14.2
8_28	0.0292 ± 0.00121	0.2192 ± 0.01946	0.0544 ± 0.00427	185.8 ± 7.6	201.3 ± 16.3
8_29	0.0298 ± 0.00108	0.2104 ± 0.01284	0.0512 ± 0.00251	189.2 ± 6.8	193.9 ± 10.8
8_30	0.0311 ± 0.00113	0.2090 ± 0.01297	0.0488 ± 0.00245	197.4 ± 7.1	192.7 ± 11.0
8_31	0.0285 ± 0.00107	0.1922 ± 0.01310	0.0489 ± 0.00279	181.3 ± 6.7	178.5 ± 11.2
8_32	0.3222 ± 0.01137	4.9633 ± 0.25515	0.1117 ± 0.00418	1800.5 ± 55.7	1813.1 ± 44.4
8_33	0.0284 ± 0.00103	0.1957 ± 0.01173	0.0499 ± 0.00239	180.8 ± 6.4	181.5 ± 10.0
8_34	0.0318 ± 0.00090	0.2185 ± 0.01810	0.0499 ± 0.00388	201.6 ± 5.6	200.6 ± 15.2
8_35	0.0312 ± 0.00092	0.1999 ± 0.01748	0.0464 ± 0.00382	198.3 ± 5.7	185.1 ± 14.9
8_36	0.0192 ± 0.00060	0.1178 ± 0.01120	0.0445 ± 0.00399	122.7 ± 3.8	113.1 ± 10.2
8_37	0.3473 ± 0.00897	5.4193 ± 0.39389	0.1132 ± 0.00769	1921.5 ± 43.1	1887.9 ± 64.3
8_38	0.0401 ± 0.00119	0.2742 ± 0.02414	0.0495 ± 0.00411	253.7 ± 7.4	246.1 ± 19.4
8_39	0.0311 ± 0.00112	0.2074 ± 0.02330	0.0484 ± 0.00515	197.1 ± 7.0	191.4 ± 19.8
8_40	0.3410 ± 0.00910	5.3949 ± 0.40069	0.1148 ± 0.00795	1891.3 ± 43.9	1884.0 ± 65.7
8_41	0.0319 ± 0.00093	0.2133 ± 0.01840	0.0485 ± 0.00394	202.3 ± 5.8	196.4 ± 15.5
8_42	0.3511 ± 0.00829	5.4921 ± 0.43416	0.1135 ± 0.00856	1939.7 ± 39.7	1899.4 ± 70.3
8_43	0.3411 ± 0.00805	5.3531 ± 0.42299	0.1138 ± 0.00858	1892.0 ± 38.8	1877.4 ± 70.0
8_44	0.3804 ± 0.00906	6.6987 ± 0.53133	0.1277 ± 0.00966	2078.3 ± 42.5	2072.4 ± 72.6
8_46	0.0289 ± 0.00073	0.1981 ± 0.01680	0.0496 ± 0.00402	183.9 ± 4.6	183.5 ± 14.3
8_47	0.0308 ± 0.00092	0.2150 ± 0.02150	0.0506 ± 0.00483	195.5 ± 5.7	197.7 ± 18.1
8_48	0.0282 ± 0.00078	0.1993 ± 0.01842	0.0512 ± 0.00452	179.4 ± 4.9	184.5 ± 15.7
8_49	0.0310 ± 0.00077	0.2109 ± 0.01769	0.0494 ± 0.00395	196.7 ± 4.8	194.3 ± 14.9
8_50	0.0311 ± 0.00076	0.2156 ± 0.01779	0.0503 ± 0.00396	197.3 ± 4.8	198.2 ± 15.0
8_51	0.3439 ± 0.00923	5.0669 ± 0.58373	0.1069 ± 0.01197	1905.4 ± 44.4	1830.6 ± 102.7
8_52	0.4537 ± 0.01214	9.8023 ± 1.12743	0.1567 ± 0.01753	2411.8 ± 54.1	2416.4 ± 111.9
8_53	0.2589 ± 0.00701	3.7651 ± 0.43500	0.1055 ± 0.01185	1484.2 ± 36.0	1585.3 ± 97.2
8_54	0.3489 ± 0.00938	5.2608 ± 0.60631	0.1093 ± 0.01225	1929.6 ± 45.0	1862.5 ± 103.4
8_55	0.3412 ± 0.00906	5.1468 ± 0.59119	0.1094 ± 0.01223	1892.5 ± 43.7	1843.9 ± 102.7
8_56	0.3271 ± 0.00895	4.9292 ± 0.57102	0.1093 ± 0.01230	1824.5 ± 43.6	1807.3 ± 102.8
8_57	0.3558 ± 0.00948	5.4242 ± 0.62355	0.1106 ± 0.01237	1962.0 ± 45.2	1888.7 ± 103.7
8_58	0.0308 ± 0.00095	0.2163 ± 0.02722	0.0510 ± 0.00622	195.3 ± 5.9	198.8 ± 23.0
8_59	0.0216 ± 0.00068	0.1531 ± 0.01961	0.0515 ± 0.00639	137.6 ± 4.3	144.7 ± 17.4
8_60	0.0287 ± 0.00096	0.1999 ± 0.02671	0.0505 ± 0.00653	182.4 ± 6.0	185.1 ± 22.9

All errors are quoted at 2σ.

Appendix Table 4 LA-ICP-MS U-Pb isotopic analytical data for separated zircons from the Wanakurasawa Unit (sample KV13-4).

Grain number	$^{206}Pb/^{238}U$			$^{207}Pb/^{235}U$			$^{207}Pb/^{206}Pb$			Age					
										$^{206}Pb/^{238}U$			$^{207}Pb/^{235}U$		
WK-1	0.0407	±	0.00120	0.2873	±	0.02119	0.0512	±	0.00346	257.2	±	7.4	256.4	±	16.9
WK-2	0.0183	±	0.00056	0.1236	±	0.00985	0.0490	±	0.00361	116.8	±	3.5	118.3	±	8.9
WK-3	0.0159	±	0.00046	0.1050	±	0.00746	0.0478	±	0.00311	101.9	±	2.9	101.3	±	6.9
WK-4	0.0162	±	0.00046	0.1120	±	0.00788	0.0503	±	0.00323	103.3	±	2.9	107.8	±	7.2
WK-5	0.0394	±	0.00111	0.2810	±	0.01920	0.0518	±	0.00322	249.0	±	6.9	251.5	±	15.3
WK-6	0.0156	±	0.00044	0.1055	±	0.00728	0.0490	±	0.00309	99.9	±	2.8	101.9	±	6.7
WK-7	0.0190	±	0.00056	0.1371	±	0.01021	0.0524	±	0.00358	121.1	±	3.5	130.5	±	9.2
WK-8	0.0164	±	0.00046	0.1131	±	0.00771	0.0499	±	0.00310	105.1	±	2.9	108.8	±	7.1
WK-9	0.0172	±	0.00059	0.1189	±	0.01137	0.0501	±	0.00447	110.0	±	3.7	114.1	±	10.4
WK-10	0.0161	±	0.00049	0.1086	±	0.00853	0.0488	±	0.00354	103.2	±	3.1	104.6	±	7.8
WK-11	0.0162	±	0.00029	0.1093	±	0.00888	0.0490	±	0.00388	103.5	±	1.8	105.3	±	8.2
WK-12	0.0167	±	0.00044	0.1146	±	0.01193	0.0497	±	0.00501	106.9	±	2.8	110.2	±	10.9
WK-13	0.0165	±	0.00031	0.1056	±	0.00887	0.0464	±	0.00380	105.4	±	1.9	101.9	±	8.2
WK-14	0.0168	±	0.00027	0.1116	±	0.00864	0.0483	±	0.00366	107.2	±	1.7	107.4	±	7.9
WK-15	0.0162	±	0.00023	0.1075	±	0.00771	0.0482	±	0.00339	103.5	±	1.4	103.7	±	7.1
WK-16	0.0177	±	0.00040	0.1111	±	0.01058	0.0456	±	0.00422	112.9	±	2.5	106.9	±	9.7
WK-18	0.0170	±	0.00029	0.1172	±	0.00930	0.0501	±	0.00388	108.4	±	1.9	112.5	±	8.5
WK-19	0.0329	±	0.00045	0.2229	±	0.01578	0.0491	±	0.00341	208.7	±	2.8	204.4	±	13.2
WK-20	0.0287	±	0.00041	0.2046	±	0.01470	0.0517	±	0.00364	182.4	±	2.6	189.0	±	12.5
WK-21	0.4871	±	0.01323	11.6467	±	0.61642	0.1734	±	0.00788	2558.0	±	57.6	2576.4	±	50.7
WK-22	0.0180	±	0.00054	0.1193	±	0.00831	0.0481	±	0.00302	115.1	±	3.4	114.4	±	7.6
WK-24	0.0163	±	0.00058	0.1029	±	0.01017	0.0457	±	0.00422	104.3	±	3.7	99.4	±	9.4
WK-25	0.0153	±	0.00044	0.1013	±	0.00642	0.0482	±	0.00272	97.7	±	2.8	98.0	±	5.9
WK-28	0.0170	±	0.00052	0.1073	±	0.00801	0.0457	±	0.00311	108.8	±	3.3	103.5	±	7.4
WK-29	0.0162	±	0.00048	0.1153	±	0.00772	0.0515	±	0.00309	103.8	±	3.0	110.8	±	7.0
WK-30	0.0159	±	0.00050	0.1055	±	0.00820	0.0483	±	0.00343	101.4	±	3.2	101.9	±	7.6
WK-31	0.0183	±	0.00064	0.1181	±	0.00892	0.0468	±	0.00313	117.0	±	4.1	113.3	±	8.1
WK-32	0.0163	±	0.00055	0.1006	±	0.00673	0.0447	±	0.00259	104.5	±	3.5	97.3	±	6.2
WK-33	0.0160	±	0.00052	0.1064	±	0.00620	0.0481	±	0.00234	102.6	±	3.3	102.7	±	5.7
WK-34	0.0180	±	0.00057	0.1225	±	0.00676	0.0492	±	0.00222	115.3	±	3.6	117.4	±	6.1
WK-35	0.0162	±	0.00057	0.1167	±	0.00863	0.0523	±	0.00341	103.5	±	3.6	112.0	±	7.9
WK-36	0.3330	±	0.01032	5.2707	±	0.25151	0.1148	±	0.00417	1852.9	±	50.1	1864.1	±	41.6
WK-37	0.0188	±	0.00068	0.1378	±	0.01090	0.0531	±	0.00373	120.3	±	4.3	131.1	±	9.8
WK-38	0.0185	±	0.00062	0.1191	±	0.00810	0.0467	±	0.00276	118.0	±	3.9	114.3	±	7.4
WK-39	0.0182	±	0.00062	0.1244	±	0.00840	0.0495	±	0.00289	116.5	±	3.9	119.1	±	7.6
WK-40	0.0158	±	0.00053	0.1001	±	0.00677	0.0458	±	0.00269	101.4	±	3.4	96.9	±	6.3
WK-41	0.0176	±	0.00047	0.1160	±	0.01034	0.0478	±	0.00407	112.4	±	3.0	111.4	±	9.5
WK-42	0.0163	±	0.00042	0.1118	±	0.00954	0.0498	±	0.00405	104.2	±	2.7	107.6	±	8.8
WK-43	0.0166	±	0.00042	0.1004	±	0.00860	0.0440	±	0.00360	105.9	±	2.6	97.2	±	8.0
WK-44	0.0163	±	0.00034	0.1061	±	0.00734	0.0474	±	0.00312	103.9	±	2.2	102.4	±	6.8
WK-47	0.0162	±	0.00034	0.1026	±	0.00711	0.0459	±	0.00303	103.7	±	2.2	99.2	±	6.6
WK-48	0.0184	±	0.00038	0.1228	±	0.00827	0.0484	±	0.00310	117.5	±	2.4	117.6	±	7.5
WK-49	0.0152	±	0.00037	0.1050	±	0.00840	0.0500	±	0.00381	97.5	±	2.3	101.4	±	7.7
WK-51	0.0170	±	0.00034	0.1083	±	0.00815	0.0464	±	0.00336	108.4	±	2.1	104.4	±	7.5
WK-52	0.0183	±	0.00038	0.1131	±	0.00888	0.0448	±	0.00339	116.9	±	2.4	108.8	±	8.1
WK-53	0.0226	±	0.00040	0.1511	±	0.01032	0.0485	±	0.00320	144.1	±	2.6	142.9	±	9.1
WK-54	0.0161	±	0.00028	0.1117	±	0.00752	0.0504	±	0.00327	102.8	±	1.8	107.5	±	6.9
WK-55	0.0165	±	0.00036	0.1100	±	0.00883	0.0484	±	0.00374	105.5	±	2.3	105.9	±	8.1
WK-57	0.0190	±	0.00048	0.1264	±	0.01160	0.0483	±	0.00426	121.2	±	3.0	120.8	±	10.5
WK-58	0.0179	±	0.00040	0.1250	±	0.01013	0.0505	±	0.00394	114.6	±	2.5	119.6	±	9.2
WK-60	0.0185	±	0.00045	0.1219	±	0.01083	0.0479	±	0.00409	117.9	±	2.8	116.8	±	9.8
WK-61	0.0156	±	0.00038	0.0929	±	0.01322	0.0431	±	0.00605	99.9	±	2.4	90.2	±	12.4
WK-62	0.0165	±	0.00043	0.1002	±	0.01458	0.0441	±	0.00632	105.4	±	2.7	97.0	±	13.5
WK-63	0.0412	±	0.00144	0.3320	±	0.05328	0.0585	±	0.00916	260.1	±	8.9	291.1	±	41.4
WK-65	0.3415	±	0.00699	5.0640	±	0.67977	0.1076	±	0.01427	1893.7	±	33.7	1830.1	±	120.7
WK-67	0.0169	±	0.00047	0.1062	±	0.01589	0.0455	±	0.00669	108.2	±	3.0	102.4	±	14.7
WK-68	0.0167	±	0.00038	0.1102	±	0.01527	0.0477	±	0.00652	107.1	±	2.4	106.2	±	14.1
WK-69	0.0157	±	0.00036	0.0957	±	0.01335	0.0442	±	0.00608	100.5	±	2.3	92.8	±	12.4

All errors are quoted at 2σ.

Appendix Table 5 LA-ICP-MS U-Pb isotopic analytical data for separated zircons from the Ichinosawa Unit (sample KV13-2).

Grain number	$^{206}Pb/^{238}U$			$^{207}Pb/^{235}U$			$^{207}Pb/^{206}Pb$			Age					
										$^{206}Pb/^{238}U$			$^{207}Pb/^{235}U$		
Ic-1	0.0171	±	0.00057	0.1102	±	0.00828	0.0467	±	0.00314	109.4	±	3.6	106.1	±	7.6
Ic-2	0.3314	±	0.01004	5.1634	±	0.28536	0.1130	±	0.00522	1845.3	±	48.8	1846.6	±	48.1
Ic-3	0.0177	±	0.00056	0.1194	±	0.00753	0.0489	±	0.00268	113.1	±	3.5	114.5	±	6.9
Ic-4	0.0187	±	0.00064	0.1153	±	0.00922	0.0446	±	0.00323	119.7	±	4.1	110.8	±	8.4
Ic-5	0.0175	±	0.00058	0.1108	±	0.00804	0.0459	±	0.00296	111.9	±	3.7	106.7	±	7.4
Ic-6	0.0464	±	0.00168	0.3408	±	0.02909	0.0533	±	0.00412	292.1	±	10.3	297.8	±	22.3
Ic-7	0.0420	±	0.00143	0.2730	±	0.02131	0.0471	±	0.00331	265.4	±	8.9	245.1	±	17.1
Ic-8	0.0173	±	0.00056	0.1155	±	0.00791	0.0484	±	0.00292	110.5	±	3.5	111.0	±	7.2
Ic-9	0.0270	±	0.00086	0.2125	±	0.01376	0.0571	±	0.00322	171.7	±	5.4	195.7	±	11.6
Ic-10	0.0159	±	0.00049	0.1006	±	0.00717	0.0459	±	0.00296	101.6	±	3.1	97.3	±	6.6
Ic-11	0.3356	±	0.00921	5.1772	±	0.26941	0.1119	±	0.00495	1865.4	±	44.6	1848.9	±	45.3
Ic-12	0.3424	±	0.00938	5.3556	±	0.27819	0.1134	±	0.00501	1898.4	±	45.2	1877.8	±	45.4
Ic-13	0.0160	±	0.00047	0.1068	±	0.00685	0.0483	±	0.00275	102.6	±	3.0	103.1	±	6.3
Ic-14	0.0182	±	0.00061	0.1486	±	0.01213	0.0592	±	0.00440	116.4	±	3.9	140.7	±	10.8
Ic-15	0.0180	±	0.00059	0.1193	±	0.00960	0.0480	±	0.00353	115.2	±	3.7	114.4	±	8.7
Ic-16	0.0175	±	0.00050	0.1166	±	0.00711	0.0483	±	0.00260	112.0	±	3.2	112.0	±	6.5
Ic-17	0.0180	±	0.00058	0.1220	±	0.00969	0.0492	±	0.00357	114.9	±	3.7	116.9	±	8.8
Ic-18	0.0172	±	0.00072	0.1192	±	0.00856	0.0501	±	0.00292	110.2	±	4.6	114.4	±	7.8
Ic-19	0.0384	±	0.00153	0.2752	±	0.01575	0.0520	±	0.00213	242.6	±	9.5	246.8	±	12.6
Ic-20	0.0182	±	0.00075	0.1227	±	0.00837	0.0490	±	0.00266	116.0	±	4.8	117.5	±	7.6
Ic-21	0.0173	±	0.00072	0.1180	±	0.00846	0.0495	±	0.00288	110.4	±	4.6	113.2	±	7.7
Ic-22	0.0166	±	0.00068	0.1084	±	0.00703	0.0474	±	0.00239	106.1	±	4.3	104.5	±	6.5
Ic-23	0.0161	±	0.00067	0.0996	±	0.00719	0.0448	±	0.00264	103.2	±	4.3	96.4	±	6.7
Ic-24	0.0161	±	0.00066	0.1092	±	0.00717	0.0493	±	0.00253	102.8	±	4.2	105.3	±	6.6
Ic-25	0.0165	±	0.00074	0.1099	±	0.00743	0.0483	±	0.00245	105.6	±	4.7	105.9	±	6.8
Ic-26	0.0155	±	0.00071	0.1024	±	0.00798	0.0480	±	0.00302	98.9	±	4.5	99.0	±	7.4
Ic-27	0.0151	±	0.00067	0.0978	±	0.00648	0.0469	±	0.00231	96.7	±	4.3	94.7	±	6.0
Ic-28	0.0162	±	0.00072	0.1058	±	0.00723	0.0473	±	0.00245	103.6	±	4.6	102.1	±	6.7
Ic-29	0.0166	±	0.00076	0.1145	±	0.00830	0.0499	±	0.00282	106.4	±	4.8	110.0	±	7.6
Ic-30	0.0167	±	0.00078	0.1101	±	0.00918	0.0477	±	0.00330	106.9	±	5.0	106.1	±	8.4
Ic-31	0.4407	±	0.01514	8.8001	±	0.49103	0.1448	±	0.00637	2353.9	±	68.1	2317.5	±	52.2
Ic-32	0.0168	±	0.00061	0.1089	±	0.00777	0.0470	±	0.00288	107.4	±	3.9	104.9	±	7.1
Ic-33	0.0164	±	0.00060	0.1129	±	0.00822	0.0501	±	0.00314	104.6	±	3.8	108.6	±	7.5
Ic-34	0.0151	±	0.00058	0.0948	±	0.00774	0.0456	±	0.00329	96.6	±	3.7	92.0	±	7.2
Ic-35	0.0179	±	0.00070	0.1161	±	0.00995	0.0470	±	0.00358	114.5	±	4.4	111.5	±	9.1
Ic-36	0.0174	±	0.00062	0.1163	±	0.00765	0.0486	±	0.00268	111.0	±	3.9	111.8	±	7.0
Ic-37	0.0163	±	0.00054	0.1081	±	0.00793	0.0481	±	0.00315	104.2	±	3.4	104.2	±	7.3
Ic-38	0.0176	±	0.00055	0.1122	±	0.00713	0.0464	±	0.00257	112.2	±	3.5	108.0	±	6.5
Ic-39	0.0164	±	0.00052	0.1078	±	0.00725	0.0478	±	0.00283	104.6	±	3.3	103.9	±	6.7
Ic-40	0.0294	±	0.00091	0.2019	±	0.01267	0.0497	±	0.00271	187.0	±	5.7	186.7	±	10.8
Ic-41	0.0183	±	0.00064	0.1206	±	0.01030	0.0477	±	0.00372	117.0	±	4.1	115.6	±	9.4
Ic-42	0.0165	±	0.00054	0.1121	±	0.00814	0.0492	±	0.00319	105.6	±	3.4	107.9	±	7.5
Ic-43	0.0177	±	0.00064	0.1145	±	0.01043	0.0468	±	0.00391	113.4	±	4.1	110.1	±	9.6
Ic-44	0.3401	±	0.01025	5.3130	±	0.30387	0.1133	±	0.00551	1887.0	±	49.5	1871.0	±	50.1

All errors are quoted at 2σ.

Appendix Table 6 LA-ICP-MS U-Pb isotopic analytical data for separated zircons from the Kumotoriyama Unit (sample KV13-14).

Grain number	$^{206}Pb/^{238}U$	$^{207}Pb/^{235}U$	$^{207}Pb/^{206}Pb$	Age	
				$^{206}Pb/^{238}U$	$^{207}Pb/^{235}U$
KM_1	0.0150 ± 0.00035	0.1003 ± 0.00761	0.0487 ± 0.00351	95.7 ± 2.2	97.1 ± 7.0
KM_2	0.0162 ± 0.00027	0.1089 ± 0.00550	0.0489 ± 0.00233	103.3 ± 1.7	105.0 ± 5.0
KM_3	0.0137 ± 0.00030	0.0996 ± 0.00688	0.0527 ± 0.00346	87.7 ± 1.9	96.4 ± 6.4
KM_5	0.0166 ± 0.00025	0.1116 ± 0.00488	0.0488 ± 0.00200	105.9 ± 1.6	107.4 ± 4.5
KM_6	0.0189 ± 0.00036	0.1316 ± 0.00758	0.0505 ± 0.00275	120.8 ± 2.2	125.5 ± 6.8
KM_7	0.0166 ± 0.00044	0.1117 ± 0.00967	0.0488 ± 0.00403	106.1 ± 2.8	107.5 ± 8.9
KM_8	0.0153 ± 0.00037	0.0993 ± 0.00802	0.0471 ± 0.00363	97.7 ± 2.4	96.1 ± 7.4
KM_9	0.0159 ± 0.00030	0.1110 ± 0.00652	0.0508 ± 0.00282	101.5 ± 1.9	106.9 ± 6.0
KM_10	0.0140 ± 0.00031	0.0958 ± 0.00681	0.0496 ± 0.00335	89.6 ± 2.0	92.9 ± 6.3
KM_11	0.0158 ± 0.00025	0.1044 ± 0.00564	0.0478 ± 0.00247	101.4 ± 1.6	100.8 ± 5.2
KM_12	0.0150 ± 0.00042	0.1046 ± 0.01003	0.0506 ± 0.00464	95.9 ± 2.7	101.1 ± 9.3
KM_13	0.0158 ± 0.00034	0.1087 ± 0.00801	0.0498 ± 0.00351	101.3 ± 2.2	104.8 ± 7.4
KM_15	0.0160 ± 0.00032	0.1083 ± 0.00755	0.0489 ± 0.00327	102.6 ± 2.1	104.4 ± 6.9
KM_16	0.0163 ± 0.00028	0.1132 ± 0.00653	0.0505 ± 0.00278	104.1 ± 1.7	108.9 ± 6.0
KM_17	0.0176 ± 0.00035	0.1257 ± 0.00854	0.0517 ± 0.00336	112.7 ± 2.2	120.2 ± 7.7
KM_18	0.0167 ± 0.00025	0.1137 ± 0.00578	0.0492 ± 0.00240	107.1 ± 1.6	109.3 ± 5.3
KM_20	0.0161 ± 0.00040	0.1211 ± 0.00995	0.0545 ± 0.00427	103.1 ± 2.5	116.1 ± 9.1
KM_21	0.0159 ± 0.00040	0.1011 ± 0.00873	0.0460 ± 0.00380	101.9 ± 2.6	97.8 ± 8.1
KM_24	0.0160 ± 0.00027	0.1082 ± 0.00569	0.0490 ± 0.00245	102.4 ± 1.7	104.3 ± 5.2
KM_25	0.0169 ± 0.00027	0.1109 ± 0.00570	0.0476 ± 0.00233	107.9 ± 1.7	106.7 ± 5.2
KM_26	0.0167 ± 0.00039	0.0986 ± 0.00795	0.0429 ± 0.00331	106.6 ± 2.5	95.5 ± 7.4
KM_27	0.0149 ± 0.00027	0.0993 ± 0.00583	0.0482 ± 0.00269	95.7 ± 1.7	96.1 ± 5.4
KM_28	0.0142 ± 0.00030	0.0929 ± 0.00651	0.0476 ± 0.00318	90.6 ± 1.9	90.2 ± 6.1
KM_29	0.0166 ± 0.00041	0.1154 ± 0.00941	0.0504 ± 0.00391	106.2 ± 2.6	110.9 ± 8.6
KM_30	0.0159 ± 0.00026	0.1033 ± 0.00530	0.0472 ± 0.00230	101.5 ± 1.6	99.8 ± 4.9
KM_31	0.0163 ± 0.00037	0.1076 ± 0.00803	0.0479 ± 0.00341	104.3 ± 2.3	103.8 ± 7.4
KM_32	0.0162 ± 0.00029	0.1095 ± 0.00616	0.0491 ± 0.00262	103.4 ± 1.8	105.5 ± 5.7
KM_33	0.0161 ± 0.00042	0.1106 ± 0.00939	0.0498 ± 0.00402	103.1 ± 2.6	106.5 ± 8.6
KM_34	0.0160 ± 0.00037	0.1015 ± 0.00774	0.0460 ± 0.00334	102.5 ± 2.3	98.2 ± 7.2
KM_35	0.0167 ± 0.00030	0.1101 ± 0.00617	0.0478 ± 0.00254	106.7 ± 1.9	106.1 ± 5.7
KM_36	0.0139 ± 0.00032	0.0932 ± 0.00694	0.0485 ± 0.00344	89.3 ± 2.0	90.5 ± 6.5
KM_37	0.0158 ± 0.00029	0.1069 ± 0.00626	0.0489 ± 0.00272	101.3 ± 1.8	103.1 ± 5.8
KM_38	0.0160 ± 0.00048	0.1064 ± 0.01075	0.0482 ± 0.00466	102.3 ± 3.1	102.6 ± 9.9
KM_39	0.0160 ± 0.00028	0.1041 ± 0.00576	0.0470 ± 0.00247	102.6 ± 1.8	100.5 ± 5.3
KM_40	0.0160 ± 0.00035	0.1112 ± 0.00802	0.0505 ± 0.00347	102.0 ± 2.3	107.0 ± 7.4
KM_41	0.0167 ± 0.00096	0.1182 ± 0.01317	0.0514 ± 0.00489	106.7 ± 6.1	113.4 ± 12.0
KM_42	0.0162 ± 0.00085	0.1032 ± 0.00790	0.0462 ± 0.00257	103.7 ± 5.4	99.7 ± 7.3
KM_43	0.0150 ± 0.00080	0.0934 ± 0.00813	0.0453 ± 0.00310	95.8 ± 5.1	90.7 ± 7.6
KM_44	0.0143 ± 0.00075	0.0892 ± 0.00691	0.0451 ± 0.00257	91.8 ± 4.8	86.7 ± 6.5
KM_45	0.0177 ± 0.00093	0.1178 ± 0.00912	0.0482 ± 0.00274	113.3 ± 5.9	113.1 ± 8.3
KM_46	0.0139 ± 0.00075	0.0872 ± 0.00768	0.0455 ± 0.00317	89.0 ± 4.8	84.9 ± 7.2
KM_48	0.0168 ± 0.00091	0.1081 ± 0.00961	0.0468 ± 0.00330	107.2 ± 5.7	104.3 ± 8.8
KM_49	0.0169 ± 0.00087	0.1119 ± 0.00779	0.0481 ± 0.00224	107.9 ± 5.5	107.7 ± 7.1
KM_50	0.0164 ± 0.00085	0.1131 ± 0.00801	0.0499 ± 0.00241	105.2 ± 5.4	108.8 ± 7.3
KM_51	0.0149 ± 0.00081	0.1064 ± 0.00907	0.0518 ± 0.00341	95.3 ± 5.1	102.7 ± 8.4
KM_52	0.0160 ± 0.00086	0.0997 ± 0.00818	0.0451 ± 0.00280	102.6 ± 5.4	96.5 ± 7.6
KM_53	0.0161 ± 0.00085	0.1080 ± 0.00799	0.0487 ± 0.00253	102.8 ± 5.4	104.2 ± 7.3
KM_54	0.0142 ± 0.00079	0.1010 ± 0.00970	0.0515 ± 0.00402	91.1 ± 5.0	97.7 ± 9.0
KM_55	0.0163 ± 0.00086	0.0996 ± 0.00747	0.0444 ± 0.00237	104.1 ± 5.4	96.4 ± 6.9
KM_56	0.0164 ± 0.00086	0.1099 ± 0.00801	0.0485 ± 0.00245	105.2 ± 5.5	105.9 ± 7.4
KM_57	0.0161 ± 0.00088	0.1089 ± 0.00974	0.0490 ± 0.00347	103.0 ± 5.6	104.9 ± 9.0
KM_58	0.0153 ± 0.00086	0.0990 ± 0.00983	0.0469 ± 0.00385	98.0 ± 5.4	95.9 ± 9.1
KM_59	0.0166 ± 0.00088	0.1115 ± 0.00834	0.0487 ± 0.00258	106.3 ± 5.6	107.4 ± 7.6
KM_60	0.0157 ± 0.00083	0.1013 ± 0.00793	0.0467 ± 0.00269	100.5 ± 5.3	98.0 ± 7.3

All errors are quoted at 2σ.

Appendix Table 7 LA-ICP-MS U-Pb isotopic analytical data for separated zircons from the Happyakudani Unit (sample KV13-13).

Grain number	$^{206}Pb/^{238}U$	$^{207}Pb/^{235}U$	$^{207}Pb/^{206}Pb$	Age	
				$^{206}Pb/^{238}U$	$^{207}Pb/^{235}U$
Hp-1	0.4238 ± 0.01323	8.7958 ± 0.54948	0.1505 ± 0.15054	2277.6 ± 60.2	2317.1 ± 58.6
Hp-2	0.3367 ± 0.01051	5.3720 ± 0.33599	0.1157 ± 0.11570	1870.9 ± 50.9	1880.4 ± 55.0
Hp-3	0.0274 ± 0.00089	0.1908 ± 0.01339	0.0504 ± 0.05042	174.5 ± 5.6	177.3 ± 11.5
Hp-4	0.3287 ± 0.01037	5.1302 ± 0.32542	0.1132 ± 0.11321	1831.9 ± 50.5	1841.1 ± 55.4
Hp-5	0.3446 ± 0.01083	5.4156 ± 0.34161	0.1140 ± 0.11397	1908.9 ± 52.1	1887.3 ± 55.6
Hp-6	0.0280 ± 0.00098	0.1953 ± 0.01627	0.0507 ± 0.05065	177.8 ± 6.2	181.2 ± 13.9
Hp-7	0.0277 ± 0.00100	0.1954 ± 0.01724	0.0511 ± 0.05111	176.3 ± 6.3	181.2 ± 14.7
Hp-9	0.3429 ± 0.01070	5.3574 ± 0.33502	0.1133 ± 0.11333	1900.4 ± 51.6	1878.1 ± 55.0
Hp-11	0.0280 ± 0.00114	0.1886 ± 0.01286	0.0488 ± 0.04883	178.1 ± 7.1	175.4 ± 11.0
Hp-13	0.0297 ± 0.00123	0.2087 ± 0.01533	0.0510 ± 0.05099	188.6 ± 7.7	192.4 ± 13.0
Hp-14	0.2961 ± 0.01196	4.6038 ± 0.30051	0.1128 ± 0.11278	1671.7 ± 59.8	1750.0 ± 56.0
Hp-15	0.3831 ± 0.01540	6.9241 ± 0.44739	0.1311 ± 0.13108	2090.8 ± 72.2	2101.7 ± 59.0
Hp-17	0.3209 ± 0.01287	5.0363 ± 0.32407	0.1138 ± 0.11383	1794.1 ± 63.1	1825.4 ± 56.0
Hp-19	0.3580 ± 0.01447	5.5887 ± 0.36489	0.1132 ± 0.11322	1972.7 ± 69.0	1914.4 ± 57.8
Hp-20	0.0277 ± 0.00113	0.1893 ± 0.01294	0.0495 ± 0.04952	176.3 ± 7.1	176.0 ± 11.1
Hp-21	0.0276 ± 0.00091	0.1923 ± 0.01624	0.0505 ± 0.05052	175.6 ± 5.7	178.6 ± 13.9
Hp-22	0.3541 ± 0.01118	5.4140 ± 0.41617	0.1109 ± 0.11090	1954.1 ± 53.4	1887.1 ± 68.1
Hp-23	0.0278 ± 0.00096	0.1987 ± 0.01807	0.0519 ± 0.05186	176.7 ± 6.0	184.0 ± 15.4
Hp-24	0.0280 ± 0.00091	0.1841 ± 0.01495	0.0476 ± 0.04764	178.2 ± 5.7	171.6 ± 12.9
Hp-25	0.3406 ± 0.01076	5.2540 ± 0.40419	0.1119 ± 0.11188	1889.5 ± 52.0	1861.4 ± 67.8
Hp-26	0.3347 ± 0.01068	5.1884 ± 0.40234	0.1124 ± 0.11242	1861.3 ± 51.8	1850.7 ± 68.3
Hp-28	0.0286 ± 0.00094	0.1902 ± 0.01604	0.0483 ± 0.04833	181.5 ± 5.9	176.8 ± 13.8
Hp-29	0.3202 ± 0.01012	4.8524 ± 0.37342	0.1099 ± 0.10990	1790.8 ± 49.6	1794.0 ± 66.9
Hp-30	0.3310 ± 0.01039	5.1152 ± 0.39141	0.1121 ± 0.11207	1843.5 ± 50.5	1838.6 ± 67.2
Hp-31	0.0272 ± 0.00081	0.1900 ± 0.01764	0.0507 ± 0.05065	173.0 ± 5.1	176.6 ± 15.2
Hp-32	0.3404 ± 0.00981	5.2450 ± 0.46922	0.1117 ± 0.11174	1888.8 ± 47.4	1860.0 ± 79.3
Hp-33	0.3368 ± 0.00971	5.1422 ± 0.46028	0.1107 ± 0.11075	1871.0 ± 47.0	1843.1 ± 79.1
Hp-34	0.0274 ± 0.00087	0.1829 ± 0.01843	0.0484 ± 0.04839	174.3 ± 5.5	170.6 ± 15.9
Hp-35	0.3374 ± 0.00986	5.2526 ± 0.47343	0.1129 ± 0.11290	1874.2 ± 47.7	1861.2 ± 79.9
Hp-36	0.3358 ± 0.00981	5.3344 ± 0.48066	0.1152 ± 0.11520	1866.6 ± 47.5	1874.4 ± 80.1
Hp-37	0.3226 ± 0.00945	5.0186 ± 0.45280	0.1128 ± 0.11282	1802.6 ± 46.2	1822.5 ± 79.4
Hp-38	0.0367 ± 0.00111	0.2530 ± 0.02412	0.0500 ± 0.05001	232.3 ± 6.9	229.0 ± 19.7
Hp-39	0.0279 ± 0.00088	0.1880 ± 0.01871	0.0488 ± 0.04882	177.6 ± 5.5	174.9 ± 16.1
Hp-40	0.3079 ± 0.00894	4.7498 ± 0.42669	0.1119 ± 0.11188	1730.4 ± 44.2	1776.1 ± 78.3
Hp-41	0.3341 ± 0.00826	5.3763 ± 0.26770	0.1167 ± 0.11671	1858.2 ± 40.1	1881.1 ± 43.5
Hp-45	0.0274 ± 0.00072	0.1896 ± 0.01130	0.0502 ± 0.05019	174.3 ± 4.5	176.3 ± 9.7
Hp-46	0.0571 ± 0.00149	0.4244 ± 0.02472	0.0539 ± 0.05392	357.9 ± 9.1	359.2 ± 17.8
Hp-47	0.0567 ± 0.00150	0.4284 ± 0.02544	0.0548 ± 0.05476	355.7 ± 9.1	362.0 ± 18.2
Hp-48	0.0348 ± 0.00090	0.2443 ± 0.01420	0.0509 ± 0.05088	220.7 ± 5.6	221.9 ± 11.7
Hp-50	0.3328 ± 0.00814	5.3408 ± 0.26225	0.1164 ± 0.11638	1852.1 ± 39.5	1875.4 ± 42.9
Hp-51	0.0274 ± 0.00068	0.1913 ± 0.01121	0.0506 ± 0.05062	174.3 ± 4.3	177.8 ± 9.6
Hp-52	0.3414 ± 0.00799	5.3976 ± 0.26928	0.1147 ± 0.11468	1893.2 ± 38.5	1884.5 ± 43.7
Hp-53	0.3295 ± 0.00782	5.2353 ± 0.26536	0.1152 ± 0.11525	1835.8 ± 38.0	1858.4 ± 44.2
Hp-54	0.3037 ± 0.00711	4.8238 ± 0.24098	0.1152 ± 0.11519	1709.7 ± 35.3	1789.1 ± 42.9
Hp-55	0.0287 ± 0.00071	0.1953 ± 0.01130	0.0493 ± 0.04933	182.4 ± 4.5	181.1 ± 9.6
Hp-57	0.0273 ± 0.00071	0.1765 ± 0.01131	0.0469 ± 0.04686	173.7 ± 4.4	165.0 ± 9.8
Hp-58	0.0397 ± 0.00095	0.2822 ± 0.01507	0.0515 ± 0.05149	251.3 ± 5.9	252.4 ± 12.0
Hp-59	0.4102 ± 0.00969	7.4537 ± 0.37452	0.1318 ± 0.13178	2215.9 ± 44.4	2167.4 ± 46.0
Hp-60	0.3511 ± 0.00842	5.4901 ± 0.28140	0.1134 ± 0.11341	1939.8 ± 40.3	1899.0 ± 45.0
Hp-61	0.3558 ± 0.00917	6.0415 ± 0.30068	0.1232 ± 0.12315	1962.2 ± 43.8	1981.8 ± 44.3
Hp-63	0.0277 ± 0.00078	0.1904 ± 0.01219	0.0499 ± 0.04986	176.1 ± 4.9	177.0 ± 10.5
Hp-64	0.0269 ± 0.00076	0.1912 ± 0.01225	0.0515 ± 0.05154	171.2 ± 4.8	177.7 ± 10.5
Hp-65	0.3305 ± 0.00852	5.1296 ± 0.25527	0.1126 ± 0.11255	1841.0 ± 41.4	1841.0 ± 43.2
Hp-66	0.3417 ± 0.00879	5.3528 ± 0.26598	0.1136 ± 0.11362	1894.8 ± 42.4	1877.3 ± 43.4
Hp-67	0.0262 ± 0.00084	0.1950 ± 0.01592	0.0541 ± 0.05406	166.5 ± 5.3	180.9 ± 13.6
Hp-68	0.0280 ± 0.00084	0.2049 ± 0.01470	0.0531 ± 0.05311	177.9 ± 5.3	189.3 ± 12.5
Hp-70	0.0298 ± 0.00084	0.2027 ± 0.01297	0.0493 ± 0.04932	189.3 ± 5.3	187.4 ± 11.0
Hp-71	0.0268 ± 0.00069	0.1750 ± 0.01964	0.0473 ± 0.04731	170.7 ± 4.4	163.7 ± 17.1
Hp-72	0.0276 ± 0.00082	0.1807 ± 0.02213	0.0474 ± 0.04741	175.8 ± 5.1	168.7 ± 19.2
Hp-73	0.3534 ± 0.00794	5.5247 ± 0.56947	0.1134 ± 0.11337	1951.0 ± 37.9	1904.4 ± 92.7
Hp-74	0.0260 ± 0.00083	0.1618 ± 0.02110	0.0451 ± 0.04513	165.5 ± 5.2	152.3 ± 18.6
Hp-75	0.3441 ± 0.00787	5.2032 ± 0.53875	0.1097 ± 0.10967	1906.3 ± 37.9	1853.1 ± 92.3
Hp-76	0.0277 ± 0.00064	0.1824 ± 0.01921	0.0478 ± 0.04778	176.1 ± 4.0	170.2 ± 16.6
Hp-77	0.0282 ± 0.00079	0.1774 ± 0.02106	0.0456 ± 0.04555	179.6 ± 5.0	165.8 ± 18.3
Hp-78	0.3401 ± 0.00766	5.1324 ± 0.52943	0.1095 ± 0.10946	1887.0 ± 37.0	1841.5 ± 91.7
Hp-79	0.0283 ± 0.00078	0.1872 ± 0.02192	0.0480 ± 0.04801	179.7 ± 4.9	174.2 ± 18.9

All errors are quoted at 2σ.